LM-03K061
June 16, 2003

Wafer Bonding and Epitaxial Transfer of GaSb-based Epitaxy to GaAs for Monolithic Interconnection of Thermophotovoltaic Devices

C.A. Wang, D.A. Shiau, P.G. Murphy, P.W. O'Brien, R.K. Huang, M.K. Connors, A.C. Anderson, D. Donetsky, S. Anikeev, G. Belenky, D.M. Depoy, G. Nichols

2003 Electronic Materials Conference
Salt Lake City, Utah
25-27 June 2003

Wafer Bonding and Epitaxial Transfer of GaSb-based Epitaxy to GaAs for Monolithic Interconnection of Thermophotovoltaic Devices

C.A. Wang, D.A. Shiau, P.G. Murphy, P.W. O'Brien, R.K. Huang, M.K. Connors, A.C. Anderson
Lincoln Laboratory, Massachusetts Institute of Technology, Lexington, MA 02420-9108
D. Donetsky, S. Anikeev, G. Belenky
State University of New York, Stony Brook, NY 11794-2350
D.M. Depoy, G. Nichols
Lockheed Martin Corporation, Schenectady, NY 12301

ABSTRACT

GaInAsSb/AlGaAsSb/InAsSb/GaSb epitaxial layers were bonded to semi-insulating GaAs handle wafers with SiO_x/Ti/Au as the adhesion layer for monolithic interconnection of thermophotovolatic (TPV) devices. Epitaxial transfer was completed by removal of the GaSb substrate, GaSb buffer, and InAsSb etch-stop layer by selective chemical etching. The SiO_x/Ti/Au provides not only electrical isolation, but also high reflectivity and is used as an internal back-surface reflector. Characterization of wafer-bonded epitaxy by high-resolution x-ray diffraction and time-decay photoluminescence indicates minimal residual stress and enhancement in optical quality. 0.54-eV GaInAsSb cells were fabricated and monolithically interconnected in series. A 10-junction device exhibited linear voltage building with an open-circuit voltage of 1.8 V.

*This work was sponsored by the Department of Energy under AF Contract No. F19628-00-C-0002. The opinions, interpretations, conclusions and recommendations are those of the author and are not necessarily endorsed by the United States Government.

INTRODUCTION

GaSb-based III-V semiconductors that are closely lattice matched to GaSb substrates and include alloys based on AlSb, GaSb, GaAs, AlAs, InAs, and InSb, are extremely attractive for high-speed, low-power electronics and mid-infrared optoelectronics. The high electron mobility of InAs and the large range of energy gaps of these materials, coupled with band alignments that can be type I or type-II staggered or broken, allow for diverse and unique devices [1]. To fully exploit the potential and functionality of these materials, it is advantageous to grow the epitaxial layers on a lattice-matched semi-insulating (SI) substrate. For example, high-speed electronic devices are grown on a SI substrate to minimize parasitic capacitance, while monolithic interconnection requires a SI substrate for device isolation. However, the small energy gap of GaSb (0.72 eV) makes it extremely difficult to produce SI GaSb substrates. The lack of their availability has thus motivated a variety of alternative solutions such as mismatched growth on specially designed buffer layers [2-4]; GaSb transfer by hydrogen implantation [5-6]; lateral epitaxial overgrowth [7]; and wafer bonding or wafer fusion followed by epitaxial transfer [8-10].

In this paper, we report wafer bonding and epitaxial transfer of GaSb-based structures to SI GaAs for monolithic series interconnection of 0.54-eV thermophotovoltaic (TPV) devices. Such interconnection allows building of open-circuit voltage, reduces parasitic resistive losses, and simplifies fabrication [11-13]. The bonding approach used here is based on metal as the adhesion layer [14-15]. Since the metal can have high reflectivity, it also serves as an internal back-surface reflector (BSR) to increase photon recycling effects. Consequently, device performance enhancements might be realized. Furthermore, the reflector could be designed so that requirements of front surface filters [16] used for spectral control might be somewhat relaxed. However, since metals are electrically conducting and can alloy to the semiconductor, an SiO_x dielectric layer was incorporated to provide electrical isolation for monolithic interconnection of TPV devices and prevent alloying. The adhesion layer consists of SiO_x/Au, and because of the low index of refraction of SiO_x, the composite layer can be designed to have a higher reflectivity than would normally be obtained from a single metal layer [10]. Figure 1 schematically illustrates the final wafer-bonded (WB) device, which consists of an electrically insulating, broad-band, high-reflectivity reflector sandwiched between the GaSb-based TPV layers and the GaAs handle wafer. Materials characterization of both WB and unbonded control

GaInAsSb/AlGaAsSb/GaSb TPV structures is reported. The effectiveness of the SiO_x/Au bonding layer as an internal BSR is evaluated by measurement of minority-carrier lifetime in WB and unbonded control AlGaAsSb/GaInAsSb/AlGaAsSb lifetime structures. Furthermore, monolithic series-interconnected TPV cells were fabricated and their performance is presented.

EXPERIMENTAL APPROACH

GaInAsSb/AlGaAsSb/GaSb epitaxial layers were grown lattice matched to 5-cm-diam GaSb substrates by organometallic vapor phase epitaxy. The energy gap of the GaInAsSb active layer was ~0.54 eV. To achieve the WB p-on-n TPV device structure shown in Figure 1, the layers were grown in a reverse sequence compared to conventional TPV structures [17-18]. In addition, an InAsSb etch-stop layer was grown to allow complete removal of the GaSb substrate and buffer layer. As-grown TPV structures for bonding consist of the following layers: u-GaSb buffer layer, u-InAsSb, p-GaSb, p-AlGaAsSb, p-GaInAsSb, n-GaInAsSb, and n-GaSb. In addition, p-on-n TPV structures without the InAsSb etch-stop layer were grown as control TPV structures. Samples for determination of minority-carrier lifetime were also grown for wafer bonding and as control samples. The double heterostructures (DHs) consist of a 1.5-μm-thick p-GaInAsSb layer doped at $2 \times 10^{17} cm^{-3}$ and AlGaAsSb cap layers. GaSb was grown on the upper AlGaAsSb layer to prevent it from oxidizing. Similarly, an InAsSb etch-stop layer was grown in the sample that was wafer bonded, while it was omitted for the control structure.

To minimize residual stress in WB epitaxy, SI GaAs was selected as the handle wafer since its thermal expansion coefficient ($\alpha = 5.7 \times 10^{-6} K^{-1}$) is closely matched to that of GaSb ($\alpha = 6.9 \times 10^{-6} K^{-1}$). After megasonically cleaning in solvents and chemically etching the epitaxial and handle SI GaAs wafers to remove native oxides, the epitaxial wafer was sputter-coated with SiO_x/Ti/Au while the GaAs wafer was sputter-coated with Ti/Au. Although Ti decreases the reflectivity, it improves Au adhesion to SiO_x. SiO_x was not deposited on the GaAs wafer since this layer increases residual stress in the WB epitaxy. The SiO_x thickness was 200 nm, while the Au thickness was 2 μm, which are thicknesses that were found to result in low residual stress [19]. To bond the wafers, the two Au surfaces were placed in contact; the wafers were heated under vacuum to a temperature of 250 °C; and a mechanical pressure of 250 psi was applied.

Epitaxial transfer was accomplished by removal of the GaSb substrate and GaSb and InAsSb etch-stop layers. The 5-cm-diam bonded wafers was first cut into four quarters for ease of

handling and processing. The bulk of the 500-μm-thick GaSb substrate was removed by spin-etching with H_2O_2:H_2O:NaK tartrate tetrahydrate, leaving about 50 μm of the substrate. The remaining substrate and GaSb buffer layer were then selectively removed using a CrO_3:HF:H_2O based etch to expose the InAsSb layer. Finally, the InAsSb etch-stop layer was selectively removed with a citric acid:H_2O_2 based etch [20].

The WB and unbonded control epitaxy, were characterized by high-resolution x-ray diffraction (HRXRD), photoluminescence (PL), and time-resolved PL [21]. WB epitaxy was processed using standard photolithographic processes [4] to fabricate monolithic series-interconnected TPV devices. The fabrication process involved multiple masking, photoresist baking, and annealing steps, and the integrity of the Au-bonded epitaxial layers was maintained throughout all processing steps.

RESULTS AND DISCUSSION

The SiO_x layer provides electrical isolation, and selection of its thickness for this study was based on a compromise between obtaining a high reflectivity in two wavelength ranges while minimizing residual stress. High reflectivity between 1.5 to 2.5 μm is desirable for enhancements in cell performance, while the range between 2.5 to 15 μm can be important for spectral control [22]. In a separate set of experiments, reflectivity measurements were made on GaAs wafers that were coated with SiO_x of various thicknesses ranging from 50 to 360 nm and Au [9]. The integrated near-normal reflectivity from 1.5 to 2.5 μm increased from 0.962, 0.97, and 0.981 for SiO_x thickness of 50, 200, and 360 nm, respectively, as expected from simulations. Reflectivity from 2.5 to 15 μm, however, decreased from 0.952, 0.943, and 0.936, for SiO_x thickness of 50, 200, and 360 nm, respectively, due to absorption between 7 and 10 μm. 200-nm-thick SiO_x layers were used for wafer bonding since this thinner layer reduced residual stress in the WB epitaxy [10].

Interferograms of WB GaInAsSb/AlGaAsSb/GaSb/GaAs before substrate removal are shown in Figure 2. The bonding/reflector layer on the GaSb epilayer consisted of 200 nm SiO_x/ 5 nm Ti/ 2 μm Au, while on the GaAs it was 5 nm Ti/ 2 μm Au. The GaSb wafer is concave and exhibits an average wafer bow of 22 μm, while the GaAs is convex with bow of 24 μm. The circular fringes and nearly symmetrical wafer bow are indicative that bonding was achieved over

the entire 5-cm-diameter area. The bow is due to residual stress in the WB wafers, which results from different thermal expansion coefficients of the SiO_x, Au, GaSb, and GaAs.

The HRXRD rocking curves for the WB GaInAsSb/AlGaAsSb/GaSb TPV device structure on a GaAs handle wafer and lattice-matched GaInAsSb/AlGaAsSb/GaSb TPV structure on a GaSb substrate are shown in Figures 3a and 3b, respectively. The diffraction intensity is lower for the WB TPV device structure since the GaSb substrate has been removed and only the epitaxial layers that were grown lattice-matched to GaSb are remaining. The diffraction peak of the WB epitaxy is only slightly broadened with full-width at half-maximum (FWHM) of 51 arc s, compared to that of the control structure with FWHM of ~30 arc s. The observation of thickness fringes in both samples is indicative of the excellent structural quality and minimal wafer curvature.

The 300 K PL spectra of the WB and control TPV structures, Figure 4, show peak emission at ~2.3 μm. The PL peak intensity of the WB TPV structure with the internal BSR is over two times greater than that of the control TPV structure. These results suggest that the optical efficiency is enhanced as a result of the internal BSR and that there is negligible material degradation after wafer bonding and substrate removal. Multiple peaks in the PL spectrum of the WB sample are due to resonant absorption, which can be seen in the spectral reflectivity plot shown in Figure 5. This resonance effect results from the destructive interference of photons reflected at the air/GaSb and GaSb/SiO_x/Ti/Au interfaces. An anti-reflection (AR) coating designed for low reflectivity between 1 and 2.5 μm was deposited on the sample, and Figure 5 shows that resonant absorption is greatly reduced in this wavelength range. However, since AR coatings are typically effective only over a narrow range, resonant absorption dominates at wavelengths greater than 2.5 μm. Such effects will reduce the efficiency of the internal BSR for spectral control [23]. The integrated reflectivity from 2.5 to 15 μm is still as high as ~ 78%. One approach to further increase the long-wavelength reflectivity would be to use a thinner layer structure, which will increase the resonant fringe spacing. However, an even more effective approach is to perform the epitaxial transfer after directly fusing the epitaxy to a SI GaAs wafer [10], and then deposit a BSR on the back of the SI GaAs wafer.

Time-resolved photoluminescence measurements were made to extract minority-carrier lifetime of p-GaInAsSb doubly capped with AlGaAsSb. Figure 6 shows the normalized PL decay for WB and control GaInAsSb DHs. Low excitation conditions were used to obtain a

single time constant, which is indicative of monomolecular recombination, and thus is characteristic of the material. The lifetime measured by PL decay τ_{PL} is more than two times higher at 85 ns for the WB sample with the internal BSR compared to the control sample with τ_{PL} = 40 ns. These results show that photons that might normally be absorbed in the substrate are reflected back to the active layer and reabsorbed, and the internal BSR is effective in increasing minority-carrier lifetime.

The bulk and interface recombination processes can be described by the following equation:

$$1/\tau_{PL} = 1/\tau_{NR} + Bp/\Phi\,(W) + 2S/W; \qquad (1)$$

where τ_{NR} is the non-radiative lifetime; B is the radiative recombination coefficient; p is the carrier concentration; $\Phi(W)$ is Asbeck's photon recycling factor [25]; W is the active layer thickness; and S is the surface recombination velocity and is assumed to be equal at both the front and back heterointerfaces. Equation 1 is valid for the low excitation conditions used here and low interfacial recombination velocity $S << D/W$; where D is the minority carrier diffusion coefficient [20]. If it is assumed that recombination is radiatively limited ($B = 5 \times 10^{-11}$ cm^{-3} [24]) and that τ_{NR} can be neglected, Φ was estimated to be 3.5 from the PL decay data. This value compares favorably with a calculation of $\Phi(W)$ using the approach developed by Asbeck [25], which is shown in Figure 7.

The external quantum efficiency of uncoated WB 0.54-eV GaInAsSb/AlGaAsSb/GaSb TPV cells is shown in Figure 8. The peak external quantum efficiency is 62%, which is comparable to that of conventional cells [26]. Figure 9 shows the short-circuit current density J_{sc} versus V_{oc} for a single junction cell and 2- and 10-junction series-interconnected cells. At $J_{sc} \sim 0.4$ A/cm^2, the single cell exhibits $V_{oc} \sim 0.2$ V. At this same J_{sc}, V_{oc} is 0.37 and 1.8 V for the 2- and 10-junction devices, respectively. These results indicate that voltage building has been achieved. At higher $J_{sc} \sim 1$ A/cm^2, V_{oc} is ~ 0.470 and 2.0 V for the 2- and 10-junction devices, respectively. The saturation of V_{oc} at high J_{sc} levels may be due to heating of the devices, which were not mounted on a heatsink. These results show significant improvement for WB TPV cells compared to the alternative approach of an AlGaAsSb cell-isolation diode, for which V_{oc} of 0.42 V for a 15-cell device was measured for 0.6-eV GaInAsSb/GaSb TPV cells [4].

The V_{oc} value for the WB single cell, however, is somewhat lower compared to previously reported values for conventional cells [18]. For those devices, a typical V_{oc} value was 0.27 V at $J_{sc} \sim 0.4$ A/cm^2. Since a lower V_{oc} corresponds to a higher saturation current, the higher current

may result from the larger perimeter/area ratio compared to previously reported cells, or from pinholes in the epitaxy. These pinholes develop during selective etching and likely originated from particulates and growth defects that puncture the epitaxy during the bonding process. Any cracks or pinholes in the InAsSb layer will compromise the epitaxial layers during selective etching.

The fill factor of the 2-junction device is about 51% at $J_{sc} \sim 0.4$ A/cm^2, and degrades to about 38% at $J_{sc} \sim 1$ A/cm^2. This degradation is related to the high series resistance in the cell-to-cell interconnections. This resistance results from the thin metal contact layer, which was less than 0.5 μm, as well as from the n-lateral conduction layer, which was etched to less than 0.1 μm in thickness. It is anticipated that the performance of these WB TPV devices can be significantly improved with improvements in the fabrication process and reduced resistance in the n-GaSb lateral conduction layer.

CONCLUSIONS

In conclusion, wafer bonding of 0.54-eV GaInAsSb/AlGaAsSb/GaSb TPV device layers to GaAs handle wafers with an electrically insulating, high-reflectivity, broad-band mirror is reported. The structural properties of the WB TPV device structures are maintained after fabrication and the internal reflector enhances the PL efficiency and minority-carrier lifetime. The WB TPV structure was fabricated to form monolithically series-interconnected TPV cells. The peak external quantum efficiency of uncoated cells is 62%, and 2- and 10-junction devices exhibit voltage building.

ACKNOWLEDGMENTS

The authors gratefully acknowledge D.R. Calawa, J. Caissie, J.W. Chludzinski, P. Foti, and C.T. Harris of MIT Lincoln Laboratory for technical assistance and P. Dutta and I. Bhat of Rensselaer Polytechnic Institute for guidance in selective etching.

REFERENCES

1. P.S. Dutta, H.L. Bhat, and V. Kumar, J. Appl. Phys. 81, 5821 (1997).
2. H.-R. Blank, M. Thomas, K.C. Wong, and H. Kroemer, Appl. Phys. Lett. 69, 2080 (1996).
3. K.G. Eyink, M.L. Seaford, T.W. Haas, D.H. Tomich, W.V. Lampert, S.D. Walck, J.S. Solomon, W.C. Mitchel, and L.F. Eastman, J. Vac. Sci. Technol. B 15, 1187 (1997).
4. M.N. Palmisiano, R.M. Biefeld, J.G. Cederberg, M.J. Hafich, and G.M. Peake, AIP Conf. Proc. 653, 305-313 (2003).
5. K.D. Hobart and F.J. Kub, Electron. Lett. 35, 675 (1999).
6. Y. Zheng, P.D. Moran, Z.F. Guan, S.S. Lau, D.M. Hansen, T.F. Kuech, T.E. Haynes, T. Hoechbauer, and M. Natasi, J. Electron. Mater. 29, 916 (2000).
7. S.S. Yi, D.M. Hansen, C.K. Inoki, D.L. Harris, T.S. Kuan, and T.F. Kuech, Appl. Phys. Lett. 77, 842 (2000).
8. P.D. Moran, D. Chow, A. Hunter, and T.F. Kuech, Appl. Phys. Lett. 78, 2232 (2001).
9. C.A. Wang, P.G. Murphy, P.W. O'Brien, D.A. Shiau, A.C. Anderson, Z.L. Liau, D.M. DePoy, and G. Nichols, AIP Conf. Proc. 653, 473-481 (2003).
10. C.A. Wang, Z.L. Liau, D.A. Shiau, and P.M. Nitishin, MRS Spring Meeting, San Francisco, April 2003.
11. N.S. Fatemi, D. M. Wilt, R.W. Hoffman, Jr., M.A. Stan, V.G. Weizer, P.P. Jenkins, O.S. Khan, C.S. Murray, D. Scheiman, and D. Brinker, AIP Conf. Proc. 460, 121-131 (1999).
12. M.W. Wanlass, J.J. Carapella, A.Duda, K. Emery, L. Gedvilas, T. Moriaty, S. Ward, and J.D. Webb, X. Wu, AIP Conf. Proc 460, 132-141 (1999).
13. R.R. Siergiej, B. Wernsmann, S.A. Derry, R.G. Mahorter, R.J. Wehrer, S.D. Link, M.N. Palmisiano, R.L. Messham, S. Murray, C.S. Murray, F. Newman, J. Hills, and D. Taylor, AIP Conf. Proc. 653, 414-423 (2003).
14. C.L. Shieh, J.Y. Chi, C.A. Armiento, P.G. Haugsjaa, and A. Negri, Electron. Lett. 27, 850-851 (1991).
15. F. Omnes, J.-C. Guillaume, G. Nataf, G. Jager-Waldau, P. Vennegues, and P. Gibart, IEEE Trans. Electron. Dev. 43, 1806-1811 (1996).
16. G.W. Charache, J.L. Egley, D.M. DePoy, L.R. Danielson, M.J. Freeman, R.J. Dziendziel, J.F. Moynihan, P.F. Baldasaro, B.C. Campbell, C.A. Wang, H.K. Choi, G.W. Turner, S.J.

Wojtczuk, P. Colter, P. Sharps, M. Timmons, R.E. Fahey, and K. Zhang, J. Electron. Mater. 27, 1038-1042 (1998).

17. C.A. Wang, H.K. Choi, G.W. Charache, IEE Proc.-Optoelectron. 147, 193-198 (2000).
18. C.A. Wang, H.K. Choi, D.C. Oakley, G.W. Charache, J. Cryst. Growth 195, 346 (1998).
19. C.A. Wang, D.A. Shiau, P.G. Murphy, P.W. O'Brien, R.K. Huang, M.K. Connors, A.C. Anderson, D.M. DePoy, and G. Nichols, MRS Spring Meeting, San Francisco, April 2003.
20. G.C. DeSalvo, R. Kaspi, and C.A. Bozada, J. Electrochem. Soc. 141, 3526-3531 (1994).
21. D. Donetsky, S. Anikeev, G. Belenky, S. Luryi, C. A. Wang, and G. Nichols, Appl. Phys. Lett., 81, 4769-4771 (2002).
22. G.W. Charache, D.M. DePoy, P.F. Baldasaro, B.C. Campbell, AIP Conf. Proc. 321, 339-350 (1996).
23. M.B. Clevenger, C.S. Murray, S.A. Ringel, R.N. Sacks, L. Qin, G.W. Charache, D.M. DePoy, AIP Conf. Proc. 460, 327-334 (1999).
24. J.M. Borrego, S. Saroop, R.J. Gutman, G.W. Charache, T. Donovan, P.F. Baldasaro, C.A. Wang, J. Appl. Phys. 89, 3753 (2001).
25. P. Asbeck, J. Appl. Phys. 48, 820 (1977).
26. C.A. Wang, C.J. Vineis, H.K. Choi, M.K. Connors, R.K. Huang, L.R. Danielson, G. Nichols, G.W. Charache, D. Donetsky, S. Anikeev, G. Belenky, AIP Conf. Proc. 653, 324-334 (2003).

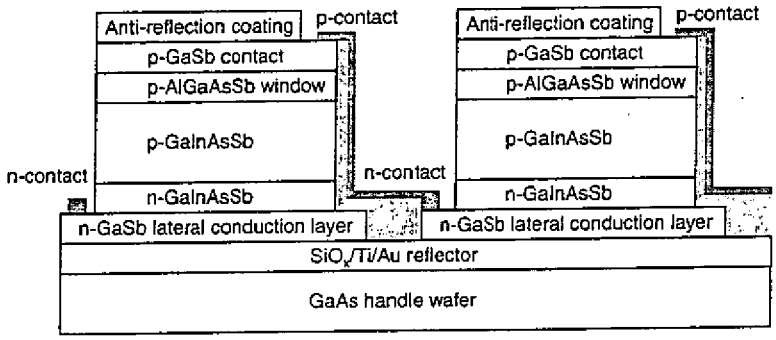

Figure 1. Schematic structure of wafer-bonded GaInAsSb/AlGaAsSb/GaSb TPV cells with monolithic series interconnections on semi-insulating GaAs handle wafer.

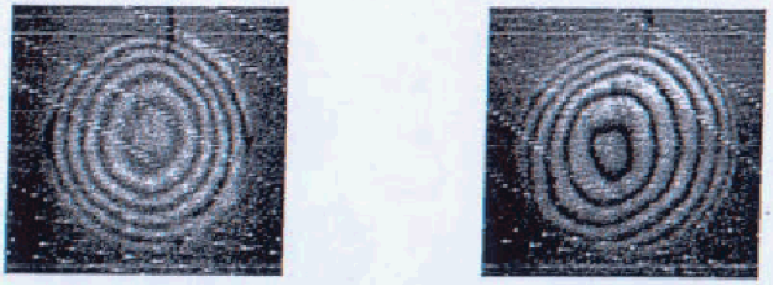

(a) (b)

Figure 2. Interferograms of (a) back side of GaSb substrate bonded to GaAs handle wafer and (b) back side of GaAs handle wafer. One fringe corresponds to 4.8 μm.

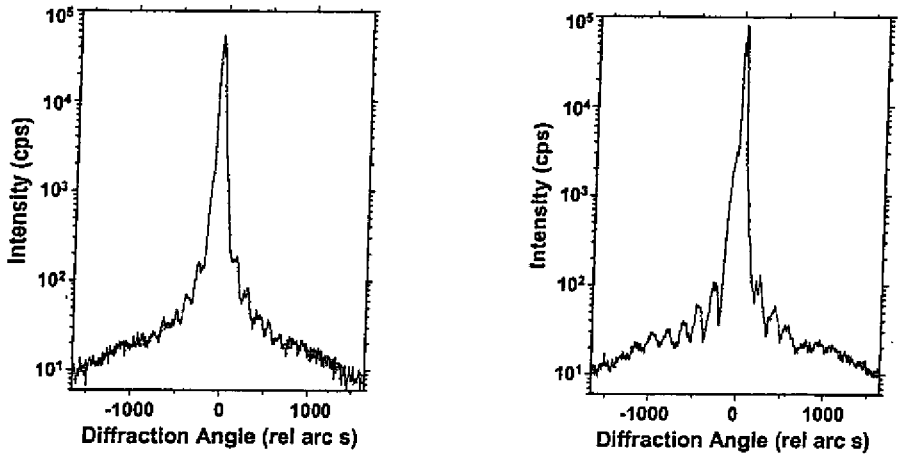

Figure 3. X-ray diffraction of 0.54-eV GaInAsSb (a) wafer-bonded TPV structure and (b) control TPV structure.

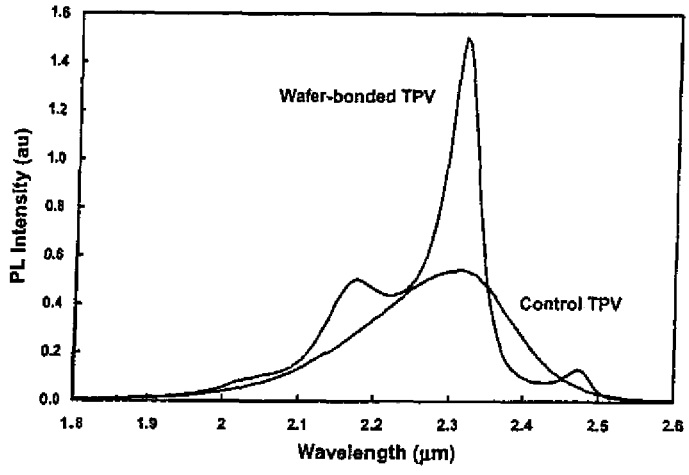

Figure 4. 300 K photoluminescence of wafer-bonded and control 0.54-eV GaInAsSb TPV structures.

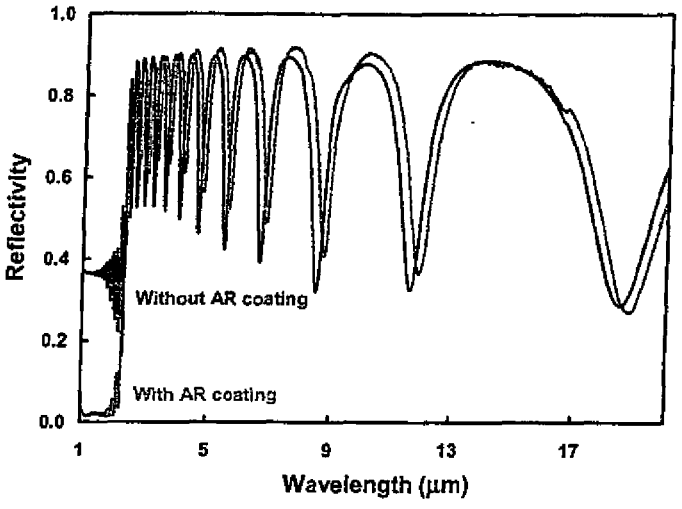

Figure 5. Reflectivity spectrum of uncoated and AR-coated wafer-bonded 0.54-eV GaInAsSb TPV structures.

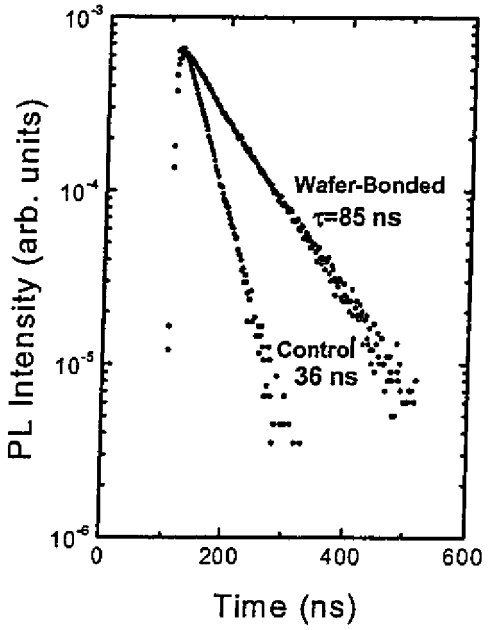

Figure 6. Photoluminescence decay of wafer-bonded and control 0.55-eV GaInAsSb lifetime structures.

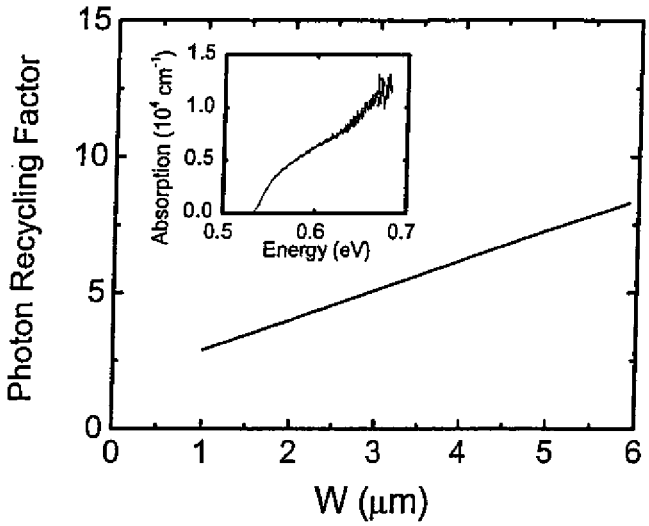

Figure 7. The calculated photon recycling coefficient for GaInAsSb versus structure thickness based on the measured fundamental absorption edge (inset).

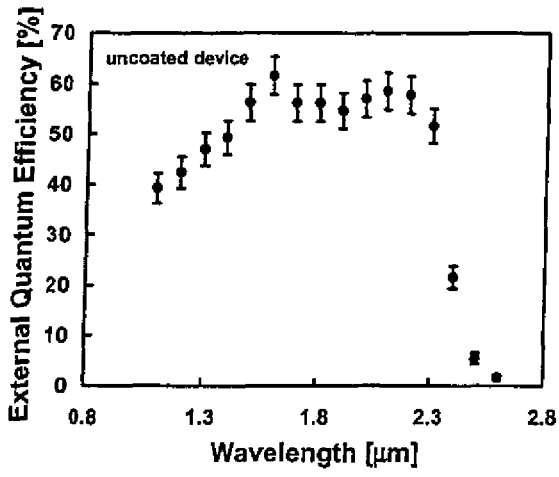

Figure 8. External quantum efficiency of uncoated wafer-bonded 0.54-eV GaInAsSb TPV device.

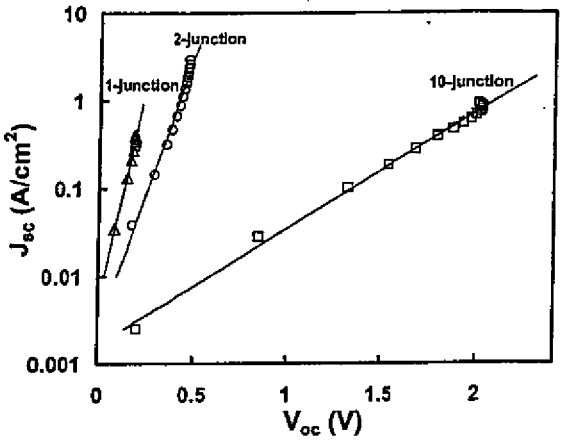

Figure 9. Semi-logarithmic plot of J_{sc} versus V_{oc} for single-junction, two-junction, and ten-junction wafer-bonded TPV 0.54-eV GaInAsSb devices.